Hindawi
Advances in Materials Science and Engineering
Volume 2017, Article ID 8175034, 11 pages
https://doi.org/10.1155/2017/8175034

Research Article

Effects of Mechanical Alloying on Sintering Behavior of Tungsten Carbide-Cobalt Hard Metal System

Ahmet Ozan Gezerman and Burcu Didem Çorbacıoğlu

Department of Chemical Engineering, Faculty of Chemical and Metallurgical Engineering, Yıldız Technical University, Istanbul, Turkey

Correspondence should be addressed to Ahmet Ozan Gezerman; ahmet_ozan@yahoo.com

Received 20 June 2017; Accepted 3 August 2017; Published 20 September 2017

Academic Editor: Peter Majewski

Copyright © 2017 Ahmet Ozan Gezerman and Burcu Didem Çorbacıoğlu. This is an open access article distributed under the Creative Commons Attribution License, which permits unrestricted use, distribution, and reproduction in any medium, provided the original work is properly cited.

During the last few years, efforts have been made to improve the properties of tungsten carbides (WCs) by preparing composite materials. In this study, we prepared WC particles by mechanical alloying and investigated the effects of mechanical alloying conditions, such as mechanical alloying time and mechanically alloyed powder ratio, on the properties of 94WC-6Co. According to experimental studies, increasing the mechanical alloying time causes an increase in the density of tungsten carbide samples and a decrease of crystal sizes and inner strength of the prepared materials. With the increase of mechanical alloying time, fine particle concentrations of tungsten carbide samples have increased. It is observed that increasing the mechanical alloying time caused a decrease of the particle surface area of tungsten carbide samples. Besides, the amount of specific phases such as Co_3W_3C and Co_6W_6C increases with increasing mechanical alloying time. As another subject of this study, increasing the concentration of mechanically alloyed tungsten carbides caused an increase in the densities of final tungsten carbide materials. With the concentrations of mechanically alloyed materials, the occurrence of Co_6W_6C and Co_3W_3C phases and the increase of crystallization are observed.

1. Introduction

Composite materials are composed of two or more materials. The properties of these materials, derived from those of the constituents, make them suitable for various applications [1, 2].

The properties of these materials, such as hardness and density, vary according to the industrial applications [3, 4]. In these studies, the density of tungsten carbide materials shows a change between 80% and 95%, while the hardness of these materials is between 580 and 1300 HV. Cemented carbides are hard and tough materials in which micrometer sized carbide particles are surrounded by a binder metal. Cemented carbides are produced by solid-state sintering of carbides and metal powders at temperatures in the range of 1300–1500°C. These materials are used under severe environmental conditions such as in the presence of abrasives (6000 revolutions at a load of 13.6 kg using a 229 mm diameter rubber wheel and dry sand) and under thermal shock (test samples were heated up to 1200°C with a heating speed of 400°C/min and cooled in water), high impact loads (3,000 kg load), and severe fatigue at temperatures as high as 1000°C. WC-Co is a hard metal cemented carbide that can be used under these conditions owing to its physical and mechanical properties. Besides the high abrasion and corrosion resistance, these materials show high temperature resistance, which is why they are used in several industries [5, 6].

In the last few years, in the electronic industry, the increased requirement of WC particles has resulted in the need for enhancing the properties of the product, such as 1500°C temperature, 500°C/min heating speed, and 4000 kg impact load [7–9]. Therefore, synthesis and sintering of WC particles have been adopted in several industries such as metal and building industries that use high temperature (>1500°C) and corrosion (95% salt spray conditions) and abrasive conditions (6000 revolutions at a load of 13.6 kg using a 229 mm diameter rubber wheel and dry sand) [10–12]. It is convenient to use WC particles with sizes in the nanometer range (<10 μm) in industrial processes such as metal industries [13–15]. Sintering below 500°C for 24 h can

afford WC particles that have a maximum particle size of 0.2 μm as pointed out by Canakci et al. and Joo et al. [16, 17]. According to these studies, at 250–450°C, decreasing of the particle size ensured obtaining materials that have more densities (<92%) at sintering temperatures (500°C). Decreasing the WC particle size has an important advantage in that it yields a large particle surface area during high-temperature processes [18]. In those studies, increasing the surface area of particles depending on the decrease of particle sizes ensured that tungsten carbide materials have higher densities (85%) at high-temperature processes (<800°C).

An increase in the carbide amount during the sintering of WC particles has a negative impact on the abrasion resistance of the resulting material [15]. In that study, the concentration of the tungsten carbide materials is 10% maximum and abrasion resistance is measured up to 1000 kg vertical load. In addition, the C/W ratio in the WC particles plays an important role in the useful properties of the final material [19].

According to this, we obtained tungsten carbide materials that have density of 90%, at C/W ratio of 20–35% and 1000 HV hardness, with 5-year corrosion resistance in salt spray testing.

In this study, the effect of sintering on a 94WC-6Co system was investigated. For preparing the powder, mechanical alloying was used for grinding, and the effects of mechanical alloying on the powders sintered using different methods were investigated.

2. Experimental Procedure

In this study, WC powder materials that contain W/C ratio of 0–7% were supplied from Eurotungstene™.

In this study, the sintering behavior, microstructure, and mechanical properties of a 94WC-6Co hard metal system produced by using mechanical alloying were investigated. The powder samples used in this study were prepared by using two different methods.

In this study, two different methods were adopted to understand the behavior of mechanically alloyed 94WC-6Co samples at different concentrations and different lengths of time.

In the first method, the effect of alloying time on mechanically alloyed 94WC-6Co powders was investigated. The powder used in the second method was obtained by adding the 94WC-6Co powder mixture mechanically alloyed for 24 h to the 94WC-6Co powder mixture that was not mechanically alloyed at different concentrations (0, 25, 50, 75, and 100%). The powders prepared by the two methods were characterized by using X-ray diffraction (XRD), scanning electron microscopy (SEM), and particle size analysis. The as-prepared cylindrical samples were uniaxially cold-pressed at 250 MPa and were sintered at 1450°C under industrial conditions. The sintered samples were characterized using XRD, SEM, and hardness measurements.

In the first method, the density values after sintering were measured for 94WC-6Co to determine physical changes. In the second method, for increasing the hardness and density, materials that were not mechanically alloyed were added to the 94WC-6Co material at different concentrations (25%, 50%, 75%, and 100%); the maximum density was obtained without the additive after 24 h mechanical alloying. Changes in the hardness and density were monitored.

Mechanical alloying was carried out at 1200 rpm using an 8000D™ Spex grinder. A WC grinder vessel and balls (6.35 mm) were used. The ball-to-powder ratio was fixed at 10 : 1. The amount of impurities added to the powder mixture from the grinder (grinder vessel and balls) was determined by weighing the powder mixture before and after alloying. In order to prevent contamination of the powder mixture during mechanical alloying, the powders were shifted to a vacuumed room (Plas-Labs™) before grinding. Ar gas was used for creating an inert atmosphere.

The mechanically alloyed powder mixtures were uniaxially pressed using a hydraulic press with 12.7 mm diameter molds at 250 MPa. All the prepared samples were sintered under vacuum at 1450°C.

The particle size distribution of all the powders was measured by using a Malvern Instruments Mastersizer 2000 apparatus. Particle size measurements were conducted in pure water supplied from a commercial Elga® device.

The powders are agitated in a Bandelin SONOREX™ ultrasonic bath to separate the agglomerated particles.

The phase analysis of the sintered samples prior to mechanical alloying was carried out by using an X-ray diffractometer (Bruker™ D8 Advance 40 kV and 40 mA) using CuKα radiation. The crystalline phases of all the green materials were identified by X-ray diffractometry (XRD) using a Bruker D8 Advanced Series diffractometer with CuKα (1.54060 Å) radiation in the 2θ range of 10–90°, with increments of 0.02° at a rate of 2°/min. International Center for Diffraction Data® (ICDD) powder diffraction files were utilized for the crystalline phase identification of the green materials. As seen in Figure 1, with the increase in the mechanical alloying time for the 94WC-6Co material, the concentrations of the Co_6W_6C and Co_3W_3C phases decreased. It is desirable to avoid the formation of these phases under the adopted reaction environment because they affect the hardness and density of the final material.

The sintered samples were placed on hot bakelite (Struers™ ThermoFast Black resin with Struers LaboPress-1 bakelite). The samples were then polished by Struers Tegrapol-15 automatic polishing device for microstructural observations and hardness measurements.

Electron backscatter diffraction (EBSD) analysis was performed for investigating the effects of mechanical alloying treatment on the material surface. EBSD patterns are generated within a small interaction volume at the surface of a sample, with a penetration depth of less than 50–100 nm. When considering how to prepare a sample for EBSD analysis, it is important to recognize that, in order to obtain high quality patterns, the surface deformation that is typically introduced during standard metallographic preparation is minimized.

On the other hand, microhardness measurements were performed after the polishing. The measurements were conducted by Vicker's test using a Shimadzu™ microhardness test device, under a load of 1000 g for a period of 15 s. For microhardness measurements, three indentations were made and measured at different points on each specimen. The average

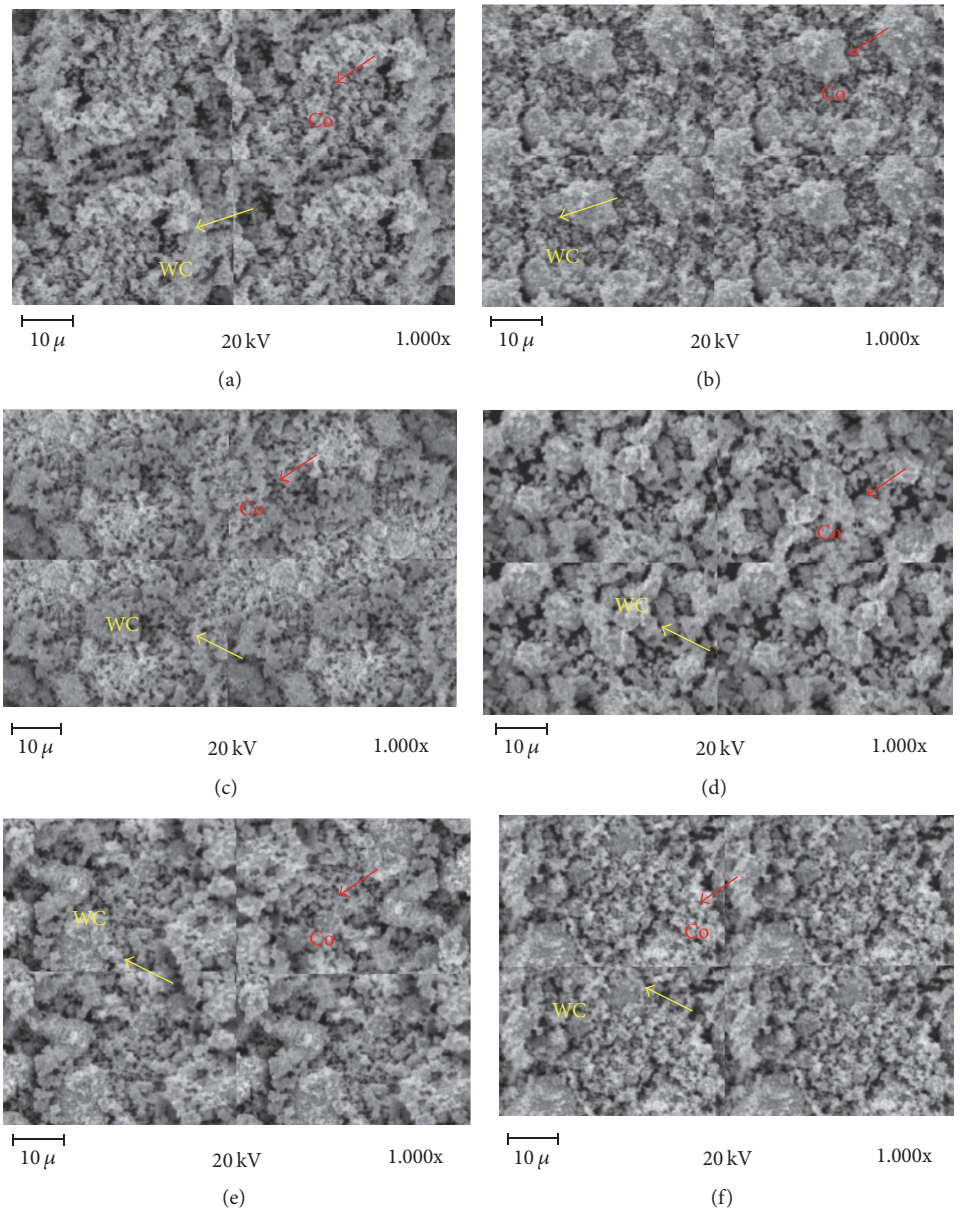


Figure 1: SEM images of the mechanically alloyed samples for (a) 20 min, (b) 1 h, (c) 3 h, (d) 6 h, (e) 12 h, and (f) 24 h.

value for each specimen was then determined. Microstructural characterization of all the precursors, mechanically alloyed powders, and sintered samples was carried out using a JEOL™ JSM-T330 electron microscope.

Scanning electron micrographs were obtained using a JEOL JSM-T330 electron microscope (SEM). Samples were prepared by placing a drop of the latex dispersion onto a brass surface, in a dust-free box at room temperature. The samples were then coated with gold, and scans were recorded at angles of 0° and 45° to the vertical direction.

3. Results and Discussion

3.1. Characterization of Powders. The powder prepared with the composition of 94WC-6Co was mechanically alloyed for different durations. The effect of mechanical alloying time on the sintered samples was investigated by observing the formation of powders and new phases and particle size distribution in the sample. The SEM images of the 94WC-6Co powders mechanically alloyed for different durations are shown in Figure 1. In the case of the powder sample subjected to mechanical alloying for 20 min, the particle size of WC decreased, and the Co particles were distributed homogeneously (Figure 1(a)). Therefore, a duration of 20 min was found to be optimum for creating homogeneous powders. The SEM images reveal that the powder mechanically alloyed for 1 h (Figure 1(b)) contained agglomerated particles, while the particles were distributed in the powder that was subjected to mechanical alloying for 3 h (Figure 1(c)). The

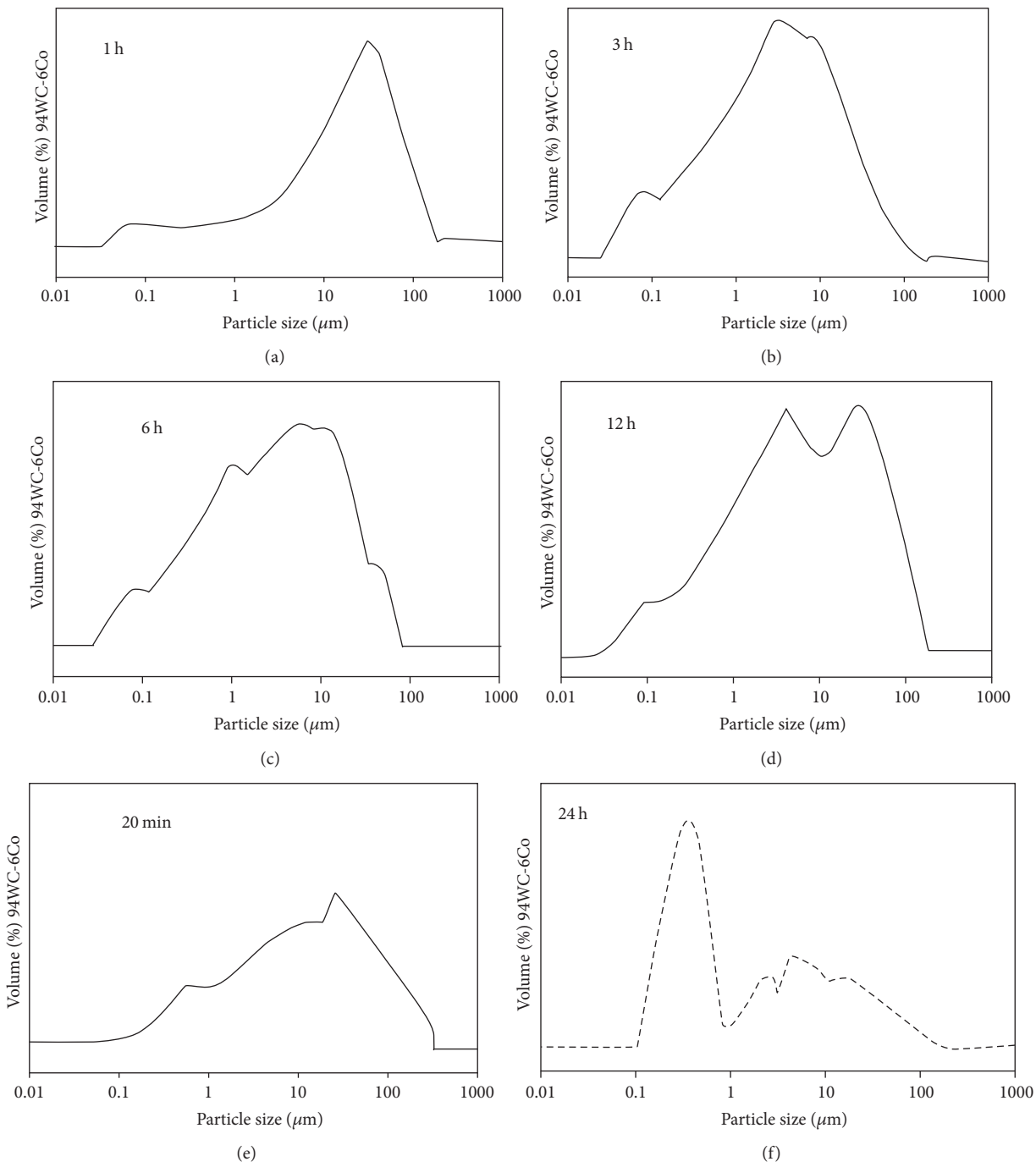


Figure 2: Particle size distribution of the powders subjected to mechanical alloying for (a) 1 h, (b) 3 h, (c) 6 h, (d) 12 h, (e) 24 h, and (f) 20 min. Comparison of the particle size distribution of the powders mechanically alloyed for 20 min, 12 h, and 24 h.

powder mechanically alloyed for 6 h (Figure 1(d)) showed the highest agglomeration. The powders subjected to mechanical alloying for 12 (Figure 1(e)) and 24 h showed similar particle distribution.

These results are also representative of the metallographic nature of the samples. The surfaces of the samples are seen in the figure.

Figure 1 also shows the microstructural formation of the WC and Co particles. The green arrow in the SEM images indicates the WC and Co particles. The larger particles comprise WC, and smaller agglomerated particles comprise the Co particles.

The particle size distributions of the mechanically alloyed powders are given in Figure 2. The average particle sizes are 13 μm, 6.3 μm, and 2.9 μm after mechanical alloying for 20 min, 12 h, and 24 h, respectively. According to these results, the average particle size of the powders decreased with increasing alloying time.

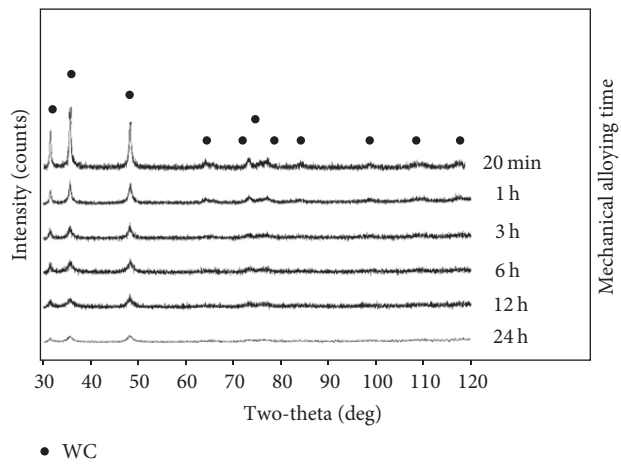


Figure 3: XRD diagrams of the powders mechanically alloyed for different durations.

None of the mechanically alloyed particles showed the formation of a new phase. The XRD patterns of the powders mechanically alloyed for different durations of time (20 min, 1 h, 3 h, 6 h, 12 h, and 24 h) are shown in Figure 3. The peak heights decreased and the peak widths increased with an increase in the mechanical alloying time, indicating that the crystal size of the powders decreased with an increase in the mechanical alloying time. As seen in Figure 3, when the mechanical alloying time increases (24 min, 1 h, 3 h, 3 h, 6 h, 12 h, and 24 h), the peak heights increased and peak widths decreased. For example, peak height for 24 min alloying is smaller than that for 1 h and the sum of the peak widths corresponding to 24 min alloying is larger than that for 1 h alloying.

The SEM images of the powders obtained by adding the 94WC-6Co powder mixture mechanically alloyed for 24 hours to the 94WC-6Co powder mixture that was not mechanically alloyed at different concentrations (25%, 50%, 75%, and 100%) are shown in Figure 4. The powder prepared by mechanical alloying for 24 h contained fine particles, although a slight degree of agglomeration was observed. In other words, according to the figure, as the concentration of the powder increases, the particle size decreases and an agglomerated structure is formed because of the increase in the number of fine particles.

An increase in the mechanical alloying time decreases the crystal size. Prolonged mechanical alloying with the effects of heat can lead to a decrease in the crystal size and increase in the surface area, so that the material properties can be controlled better.

By using SEM images of the WC particles in the second method, the particle effects on the samples were investigated. Mechanically alloyed 94WC-6Co particles at different concentrations (25%, 50%, 75%, and 100%) are shown in Figure 4. Because mechanical alloying for 24 h is sufficient for decreasing the particle size, all the powder mixtures prepared by using the second method have fine particles that result in an agglomerated structure. According to Figure 4, with an increase in the number of fine particles, the powder concentration increases, particle size decreases, and an agglomerated structure is formed. The particle sizes obtained for different mechanical alloying times are shown in Figure 2. According to these data, with increasing alloying time, the particle size distribution decreases.

3.2. Characterization of Sintered Samples

3.2.1. Effect of Mechanical Alloying Time on Sintered Samples. In this method, the effect of the mechanical alloying time on the sintering behavior of the 94WC-6Co powder mixtures was investigated. Figure 5 shows the effect of mechanical alloying on the density of the powders. With an increase in the mechanical alloying time, the size distribution of the powders decreased and their surface area increased. Hence, their green density decreased with an increase in the mechanical alloying time. The powders mechanically alloyed for 6, 12, and 24 h showed final condensation.

Figure 5 shows the effect of mechanical alloying time on the density values. With an increase in the alloying time, the particle size and density of the powder decrease but the surface area increases. The density of the samples sintered for 6, 12, and 24 h indicated full condensation. Besides, according to Figure 5, the green density reaches the maximum value (100.46%) and then decreases suddenly, which leads to abrupt changes in the microstructure, such as cracking.

The green densities of the pressed samples were determined by measuring the volumetric sizes. The Archimedes method was used for measuring the densities of the sintered samples. In this method, the samples were weighed first in air and then in liquid; the difference between the two weights was multiplied by the liquid density. In this study, to prevent oxidation, ethyl alcohol was used as the liquid.

The SEM images of the sintered 94WC-6Co samples mechanically alloyed for different durations are shown in Figure 6. The sample mechanically alloyed for 20 min contained fine particles. The mechanically alloyed samples had bigger particles as compared to the samples that were not mechanically alloyed (Figure 6(a)), and had a conventional hard metal structure [20]. The WC particles in the sample mechanically alloyed for 12 h grew in a direction different from those in the sample mechanically alloyed for 24 h (Figures 6(b) and 6(c)).

Because of the prolonged mechanical alloying (12 h, 24 h) with heating, it is reasonable to expect the WC-Co particles to move in different directions. The motion of the particles in different directions (Figures 6(c) and 6(d)) during mechanical alloying provided the desired level of hardness to the sample. In other words, movement in these directions increases the material hardness.

Note that the directions between the particles are evident for these three alloying times (20 min, 12 h, and 24 h); hence, the corresponding SEM images have been considered.

The XRD patterns of the samples mechanically alloyed for different durations are shown in Figure 7. In the case of the sample mechanically alloyed for 20 min, the Co_6W_6C and Co_3W_3C phases were not observed. As the mechanical alloying time increased, the formation of the CO_6W_6C phase increased. The Co_6W_6C and Co_3W_3C phases were observed only in the sample mechanically alloyed for 24 h, because of

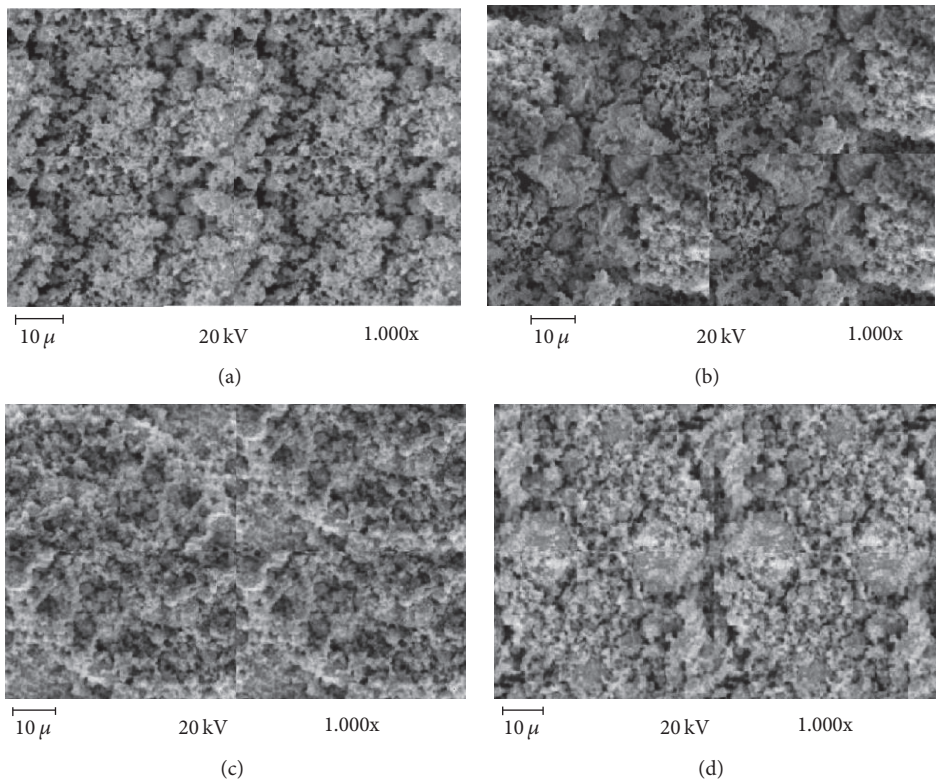


Figure 4: SEM images of the powders prepared by mechanical alloying for 24 h at different concentrations: (a) 25%, (b) 50%, (c) 75%, and (d) 100%.

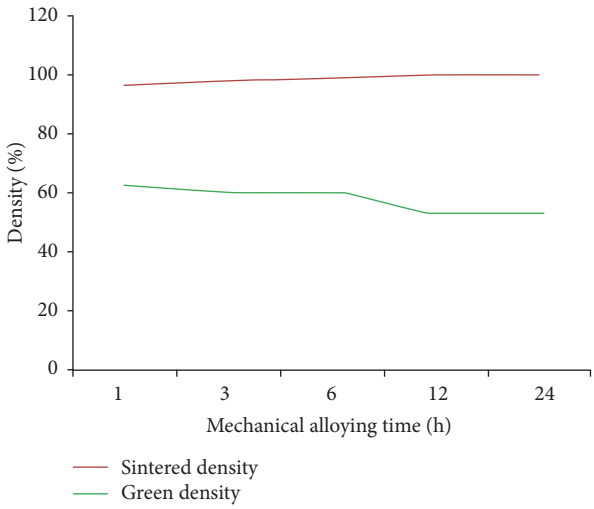


Figure 5: Variation in the green and sintered densities with mechanical alloying time.

the oxygen contamination during the mechanical alloying. Oxygen removes carbon from the samples during sintering, thus resulting in the formation of these phases by decreasing the C/W ratio [20]. The XRD patterns and SEM images reveal that the Co_6W_6C and Co_3W_3C phases contained WC particles that grew in the same direction. Therefore, the difference in the carbon concentration in the samples mechanically alloyed for 24 h led to the variation in their microstructures.

The results of the hardness analysis (Figure 8) suggest that the hardness of the samples increased with an increase in the mechanical alloying time.

As per the aim of this study, the density and hardness of the material were determined. From the data in Figures 5 and 8, the expected and desired density and hardness values were obtained. Moreover, because the concentration of agglomerated fine particles during sintering and their densities increased, the material hardness is expected to increase. As seen in Figure 3, with an increase in the mechanical alloying time for the 94WC-6 Co material, the concentrations of the Co_6W_6C and Co_3W_3C phases decrease. Because these phases affect the hardness and density of the material, their formation under the given reaction conditions must be suppressed.

According to the sintering data in Figure 5, increasing the mechanical alloying time causes an increase in the density and hardness of the material, as expected. As mentioned above, the density of the material increases with an increase in the alloying temperature and alloying time; this is because if mechanical alloying is continued after cracking of the microstructure, the hardness of the material decreases, so that the high density does not have any positive effect on the material properties.

3.2.2. Effect of Powder Concentration on Sintered Samples. In this method, the effect of powder concentration on the sintered samples subjected to mechanical alloying for 24 h was investigated. From the XRD patterns of the powder samples

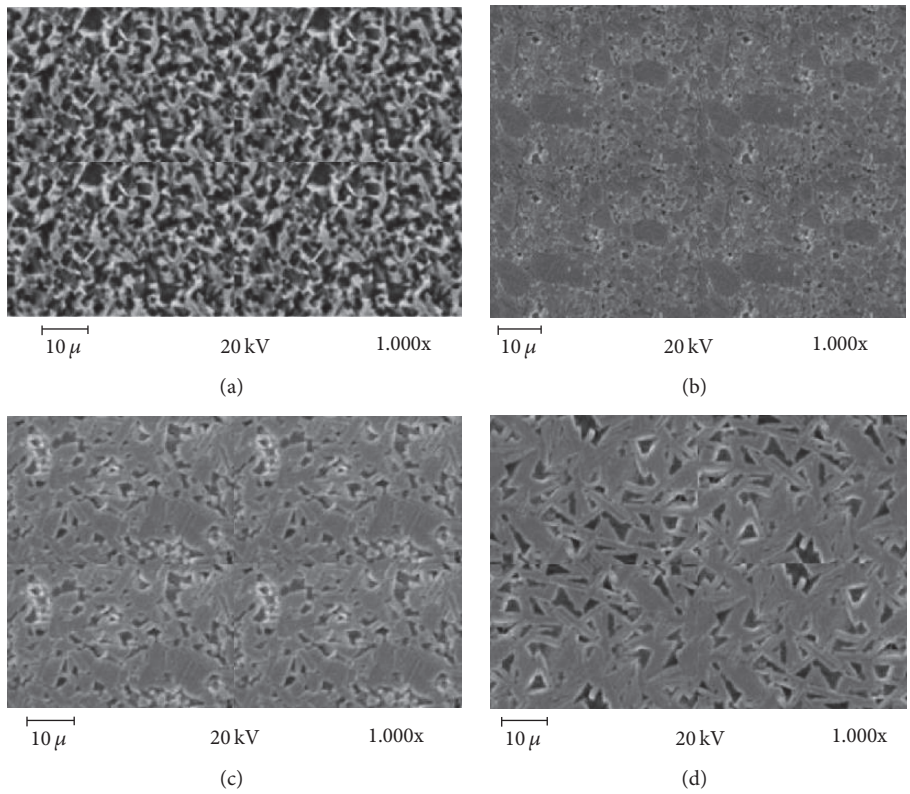


Figure 6: (a) SEM images of the unalloyed sample. SEM images of the samples sintered for different mechanical alloying times: (b) 20 min, (c) 12 h, and (d) 24 h.

mechanically alloyed for 24 h, it can be seen that as the crystal size of the powders decreased, the peak height decreased significantly, while the peak width increased. Also, because a higher density was obtained after mechanical alloying for 24 h, this alloying time is adopted for studying the effect of powder concentration on the material characteristics. For sintering processes, the samples were prepared by pressing under 250 MPa and heating at 1450°C. In the first-level experiments, the effect of alloying time on the green and sintered densities of the prepared 94WC-6Co samples was verified. Since the highest density was obtained after alloying for 24 h, this alloying time was adopted in the second-level experiments, wherein different amounts of nonmechanically alloyed 94WC-6Co were added to the 94WC-6Co samples alloyed for 24 h. The green densities and sintering densities were determined after alloying for 1, 3, 6, and 12 h without the use of additives. The maximum density was observed in the case of the sample alloyed for 24 h with 0% additive. The rate of change of density was better controlled for the samples to which different concentrations of 94WC-6Co powders (0, 25, 50, 75, and 100%) were added and alloyed for 24 h. According to XRD results (Figure 9), the width of the peak for the Co_3W_3C phase in the sample containing the 94WC-6Co powder (25%) mechanically alloyed for 24 h decreased as the sample began to crystallize. The Co_3W_3C phase is created only after 100% mechanical alloying of 94WC-6Co for 24 h. The amount of mechanically alloyed powder in this sample was greater than that in all the other samples. When the mechanical alloying time increased, the oxygen contamination also increased. Therefore, the carbide concentration was reduced significantly. The XRD patterns revealed that the Co_6W_6C phase was created before the loss of carbide. The decrease in the carbide concentration allowed the formation of the Co_3W_3C phase. The main materials used initially and the required additives are placed in a mixer and grinder. A vibrating shaft grinder was used. Powders are ground in order to separate the agglomerated particles and minimize the particle size. The grinder type can be chosen as required, and the rotation speed, ball diameter, powder-to-ball ratio, and hard metal content can be optimized. In the final stage of the grinding operation, the particle size used in the industry is 0.5–1.0 μm; it decreases to 100–150 nm when using more specific grinders. Although a wide range of particle sizes can be obtained upon grinding, with this method, the prepared mixture is essentially homogeneous, and particle agglomeration would not occur during sintering. Because the highest hardness (Figure 10) and density were obtained after 24 h of mechanical alloying, we studied the 24 h alloyed samples in the second method (Figure 11).

The XRD patterns of the sintered samples are shown in Figure 9. The peak width of the Co_6W_6C phase in the sample (mechanically alloyed for 24 h) containing 25% (w/w) 94WC-6Co increased with an increase in the mechanical alloying time.

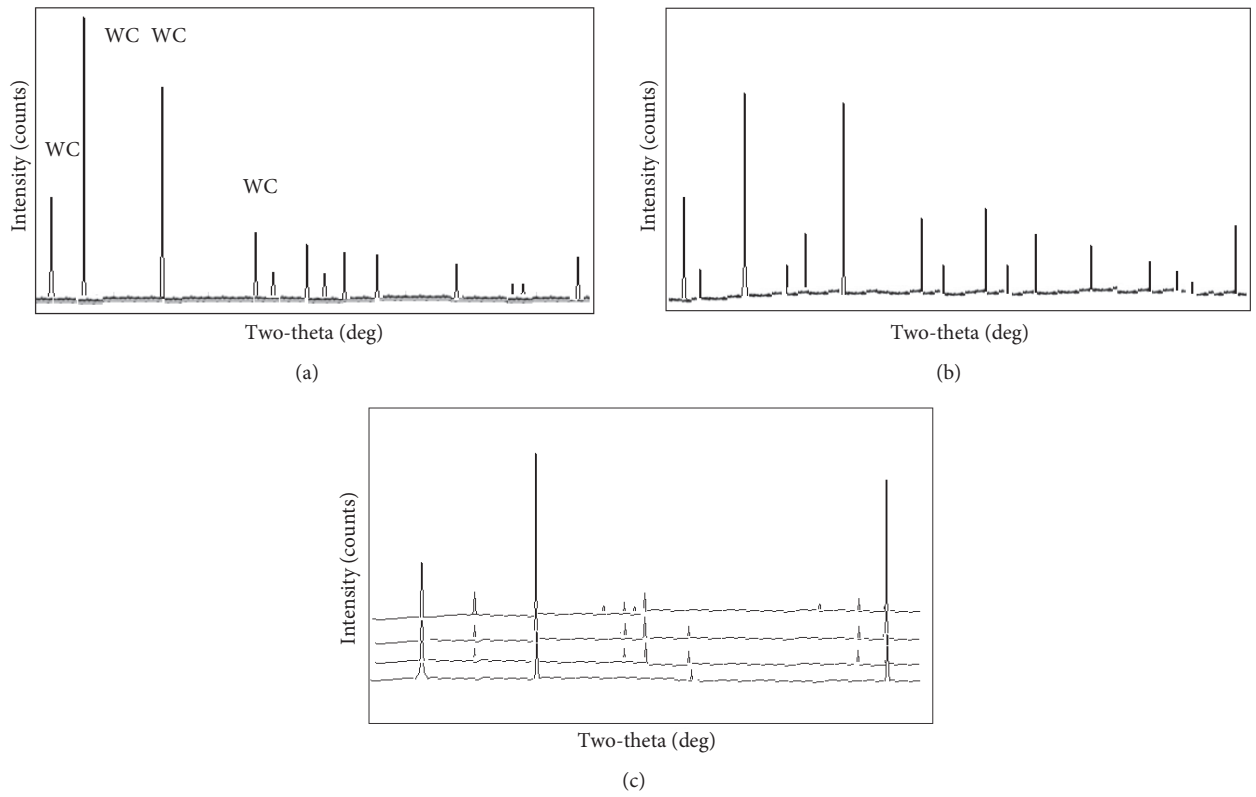


Figure 7: XRD patterns of the sintered samples mechanically alloyed for (a) 20 min and (b) 24 h; (c) comparison of the samples mechanically alloyed for 1, 3, 6, and 24 h.

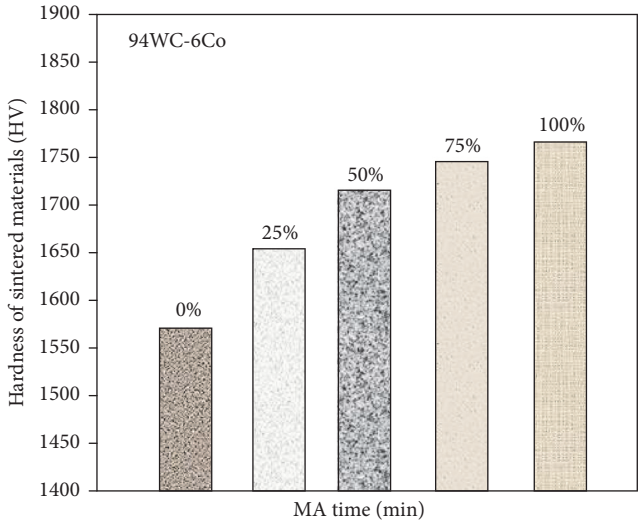


Figure 8: Hardness analysis of the sintered samples.

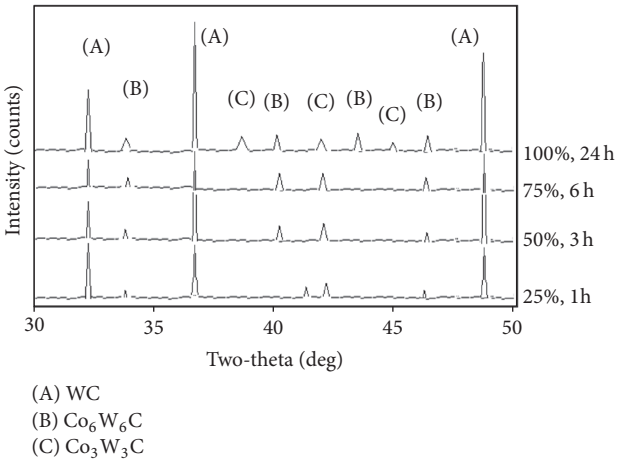


Figure 9: XRD patterns of the sintered samples.

The SEM images of the sintered samples with varying concentrations are shown in Figure 12. The sample (mechanically alloyed for 24 h) containing 0% powder was obtained by grinding the precursor powders with the sample mechanically alloyed for 20 min. The SEM image (Figure 12(a)) and XRD pattern of the sample containing 0% powder subjected to mechanical alloying for 24 h reveal the presence of 1–3 μm sized WC particles in the sample. All the observed particles were WC phases. The samples containing 25 and 0% mechanically alloyed powders (Figure 12(b)) had similar structures. With an increase in the concentration of the mechanically alloyed powders, the WC concentration decreased. The XRD patterns reveal that the Co_6W_6C phase was created in the samples containing 50% (Figure 12(c)) and 75% (Figure 12(d))

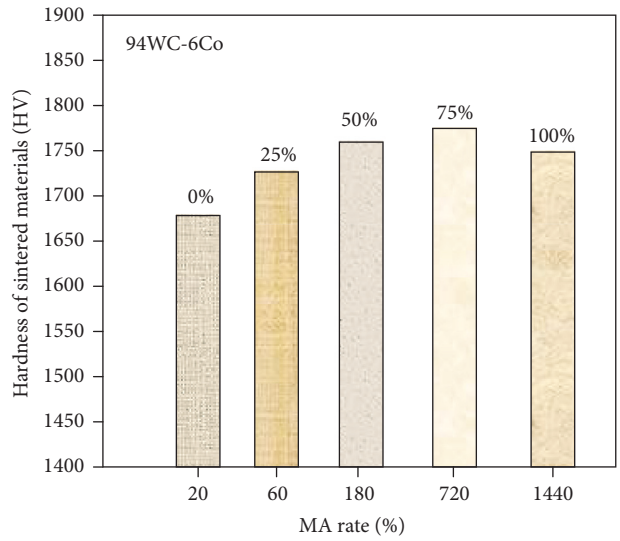


Figure 10: Hardness measurements of the sintered samples with varying concentrations of mechanically alloyed powders.

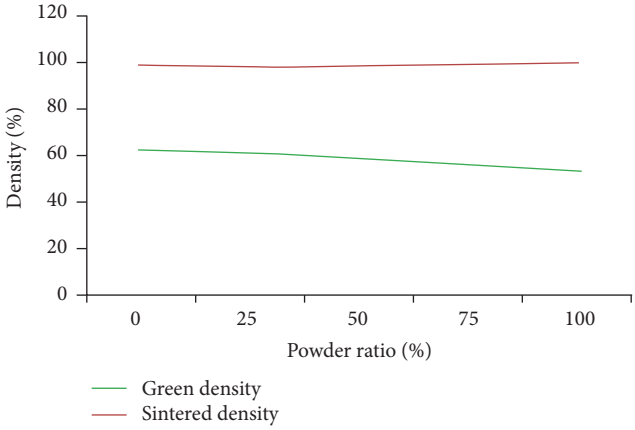


Figure 11: Relative density values of the prepared samples at different powder concentrations at a 24 h mechanical alloying time.

mechanically alloyed powder. The C/W ratio that causes the formation of this phase affects the formation of WC. In the sample containing 100% mechanically alloyed powder (Figure 12(e)), the growth of WC particles (light grey) was observed. On the basis of these results, it can be concluded that an increase in the mechanical alloying ratio affects the density positively. It was also found that the carbide concentration affected the microstructure of this system significantly.

In this method, the effect of powder concentration on the sintering behaviors of the samples mechanically alloyed for 24 h was investigated. In the first method (effect of mechanical alloying time on the sintered samples), the XRD patterns of the powder samples mechanically alloyed for 24 h revealed that the peak height decreased significantly and the peak width increased with a decrease in the crystal size of the powder. The 94WC-6Co samples were prepared using the beginning powders at different concentrations and equal composition of the powder mechanically alloyed for 24 h. The powders so prepared were pressed at 250 MPa followed by sintering at 1450°C.

The sample containing 0% powder and mechanically alloyed for 24 h was prepared using the initial powder that was alloyed for 20 min. The sample containing 0% powder contained 1–3 μm sized WC particles. All the observed particles were in the WC phase. The samples with 25 and 0% mechanically alloyed powder had similar microstructures. The samples containing 50 and 75% mechanically alloyed particles experienced deformation with an increase in the concentration of the mechanically alloyed powder and had the Co_6W_6C phase.

The formation of the Co_6W_6C phase, which depended upon the C/W ratio, led to the formation of WC particles. In the sample containing 100% mechanically alloyed powder, the WC particles grew in a detected way. On the basis of the results obtained, we can state that the increasing mechanical alloying ratio affected the density values positively. Moreover, the carbide concentration significantly affected the microstructure of this system. With an increase in the concentration of the mechanically alloyed powder, the hardness of the samples also increased.

4. Conclusions

In this study, an increase in the mechanical alloying time resulted in a decrease in the peak height and an increase in the peak width of the XRD peaks of the samples. The increase in the mechanical alloying time resulted in a decrease in the crystal size and internal strength of the powders, thus causing deformation.

With an increase in the mechanical alloying time (especially after 24 h), the fine particle concentration increased, and agglomeration between the fine particles was observed. The SEM images of the powders revealed that the particle size decreased with an increase in the mechanical alloying time.

The green density of the samples decreased with an increase in the mechanical alloying time, because of the decrease in the surface area of the powders with an increase in the mechanical alloying time. With an increase in the mechanical alloying time, the particle size of the powders decreased, while their surface area increased. The formation of the Co_3W_3C phase was observed in all the sintered samples. When mechanical alloying was carried out for 24 h, the Co_6W_6C phase was also created along with the Co_3W_3C phase.

The sample containing the powder mechanically alloyed for 20 min had fine WC particles. With an increase in the mechanical alloying time, a change in the size of the WC particles was observed. It was also found that when the concentration of the mechanically alloyed powder (24 h) increased, the green density of the samples decreased, while their sintered densities increased. The phase analysis of the samples revealed that the concentration of the Co_6W_6C phase in the sample containing mechanically alloyed powder (24 h mechanical alloying) increased as the ratio of the mechanically alloyed powder increased from 25 to 50–75% and started crystallizing. In the sample containing the powder

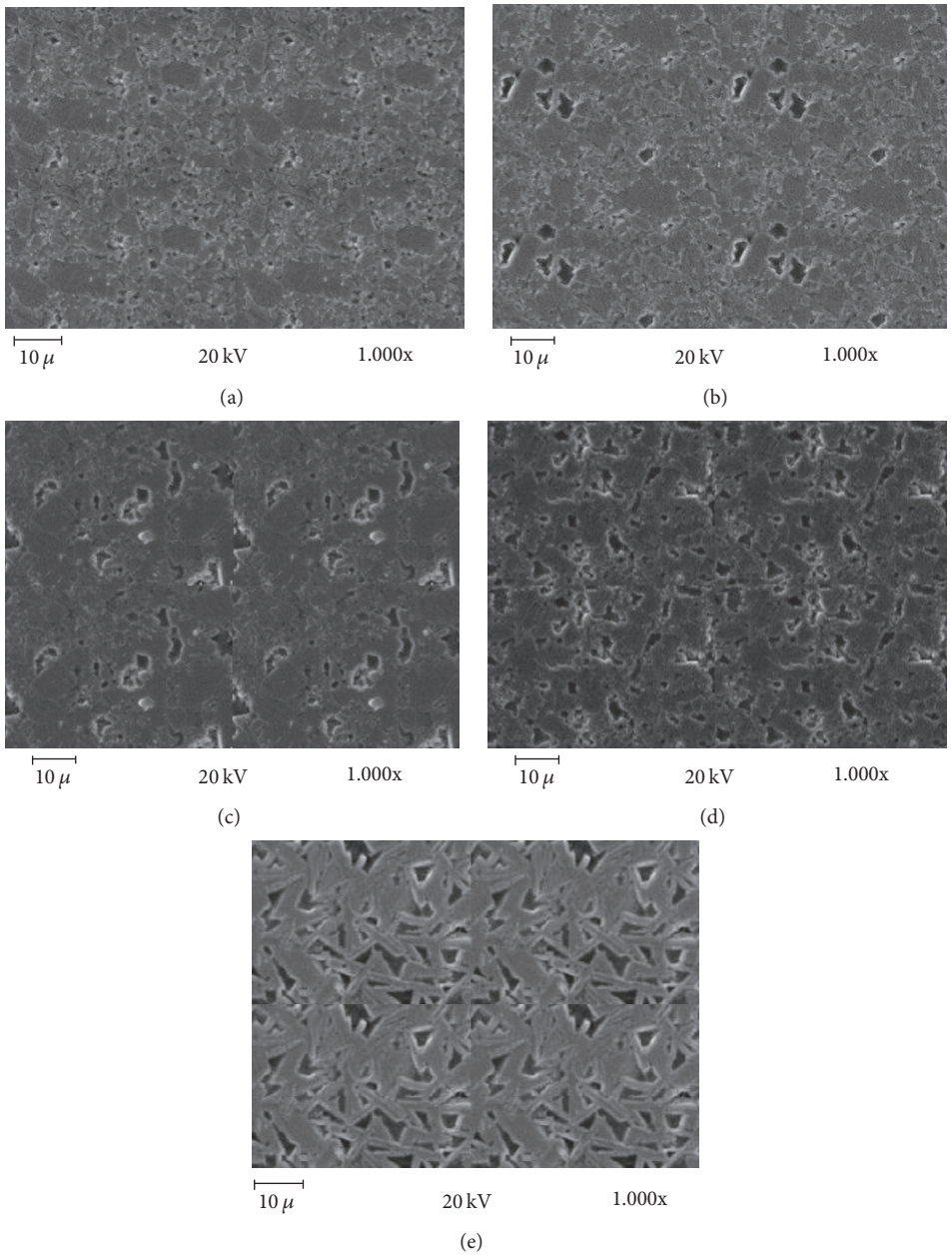


Figure 12: SEM images of the sintered samples with varying concentrations of mechanically alloyed powder: (a) 0, (b) 25, (c) 50, (d) 75, and (e) 100%.

mechanically alloyed for 24 h, both the Co_6W_6C and the Co_3W_3C phases were formed, and their XRD peaks were intense and narrow, indicating that the crystal size of both of these phases increased.

The SEM images of the powder samples that were mechanically alloyed for 24 h showed that WC particles were deformed at 0 and 25% powder concentration. The WC particles in the sample containing 100% mechanically alloyed powder grew in a given direction.

Conflicts of Interest

The authors declare that there are no conflicts of interest regarding the publication of this article.

Acknowledgments

The authors would like to thank Sabahattin Gezerman for his technical support.

References

[1] L. A. Carlsson, F. A. Donald, and R. B. Pipes, "Analysis of composite materials," in *Experimental Characterization of Advanced Composite Materials*, CRC Press, Boca Raton, Fla, USA, 2014.

[2] G. Daniel, "Composite materials: interest and physical properties," in *Composite Materials: Design And Applications*, CRC press, Boca Raton, Fla, USA, 2014.

[3] T. Louis, *Refractory Materials: A Series of Monographs ,Transition Metal Carbides And Nitrides*, University of Minnesota, New York, NY, USA, 1971.

[4] R. M. Raihanuzzaman, Z. Xie, S. J. Hong, and R. Ghomashchi, "Powder refinement, consolidation and mechanical properties of cemented carbides—an overview," *Powder Technology*, vol. 261, pp. 1–13, 2014.

[5] G. Wahl, P. B. Davies, R. F. Bunshah et al., *Ullmann's Encyclopaedia of Industrial Chemistry, Thin Films*, VCH Publishers, Weinheim, Germany, 2014.

[6] J. Yang, M. Odén, M. P. Johansson-Jõesaar, and L. Llanes, "Grinding effects on surface integrity and mechanical strength of WC-Co cemented carbides," *Procedia CIRP*, vol. 13, pp. 257–263, 2014.

[7] O. S. Manakova, A. E. Kudryashov, and E. A. Levashov, "On the application of dispersion-hardened SHS electrode materials based on (Ti, Zr)C carbide using electrospark deposition," *Surface Engineering and Applied Electrochemistry*, vol. 51, no. 5, pp. 413–421, 2015.

[8] X. Zhuang, Y. Zhang, Y. Zhu et al., "The effects of Pd and/or Zr additives on the structures and cyclic stabilities of $Mg_{50}Ni_{50}$-based electrode alloys," *International Journal of Hydrogen Energy*, vol. 40, no. 6, pp. 2768–2774, 2015.

[9] W. H. Zhong, B. Li, R. G. Maguire et al., *Synthesis, Manufacturing and Industry Impacts, Nanoscience and Nanomaterials*, DEStech Publications, Lancaster, Pa, USA, 2012.

[10] I. Konyashin and B. Ries, "Wear damage of cemented carbides with different combinations of WC mean grain size and Co content. Part I: ASTM wear tests," *International Journal of Refractory Metals and Hard Materials*, vol. 46, pp. 12–19, 2014.

[11] B. Yaman and H. Mandal, "Wear performance of spark plasma sintered Co/WC and cBN/Co/WC composites," *International Journal of Refractory Metals and Hard Materials*, vol. 42, pp. 9–16, 2014.

[12] J. Oberste-Berghaus, S. Bouaricha, J. G. Legoux, C. Moreau, and B. Harvey, "Method and apparatus for fine particle liquid suspension feed for thermal spray system and coatings formed therefrom," U.S. Patent 8,629,371, 2014.

[13] A. Jiang, Q. Li, and F. Yang, "Effects of combined addition of Cr_3C_2 and Nbc on microstructure and properties of cemented carbides prepared by WC-Co composite powder," *Materials Science Forum*, vol. 849, pp. 794–800, 2016.

[14] Y. A. Kukushkina, V. V. Sokolov, and M. V. Tomkovich, "Nanoporous carbon prepared by thermochemical treatment of carbide with chlorine," *Russian Journal of Applied Chemistry*, vol. 87, no. 10, pp. 1517–1523, 2014.

[15] I. Konyashin, S. Hlawatschek, B. Ries, F. Lachmann, and M. Vukovic, "Cobalt capping on WC-Co hardmetals. Part I: a mechanism explaining the presence or absence of cobalt layers on hardmetal articles during sintering," *International Journal of Refractory Metals and Hard Materials*, vol. 42, pp. 142–150, 2014.

[16] A. Canakci, T. Varol, H. Cuvalci, F. Erdemir, S. Ozkaya, and E. D. Yalcin, "Synthesis of novel CuSn10-graphite nanocomposite powders by mechanical alloying," *Micro and Nano Letters*, vol. 9, no. 2, pp. 109–112, 2014.

[17] H. G. Joo, D. Q. Zhang, L. X. Gao, T. Liu, and K. Y. Lee, "Corrosion resistance of tungsten carbide-based cermet coatings formed by sinter-brazing," *International Journal of Surface Science and Engineering*, vol. 8, no. 4, pp. 380–391, 2014.

[18] H. Rana, G. Shree, and A. Panwar, "Optimization of abrasive wear characteristics of tungsten carbide and chromium carbide based coating on H-13 steel using detonation gun process by taguchi method," *International Journal of Advanced Materials Manufacturing and Characterization*, vol. 1, no. 1, article 121, 2014.

[19] V. Bounhoure, S. Lay, F. Charlot, A. Antoni-Zdziobek, E. Pauty, and J. M. Missiaen, "Effect of C content on the microstructure evolution during early solid state sintering of WC-Co alloys," *International Journal of Refractory Metals and Hard Materials*, vol. 44, pp. 27–34, 2014.

[20] D. Peştreli, "Effect of mechanical alloying on the sintering behaviour of Wc-co hardmetal system [M.Sc Thesis]," Tech. Rep., Istanbul Technical University, Institute of Science and Technology, Istanbul, Turkey, 2009.



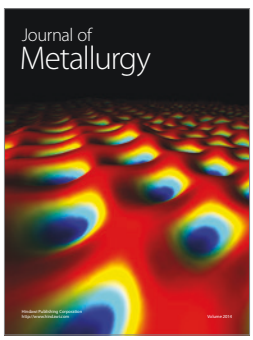




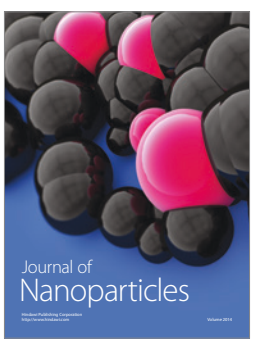


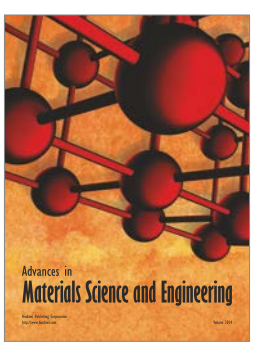


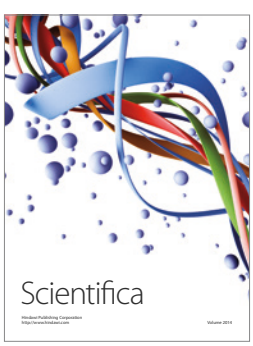


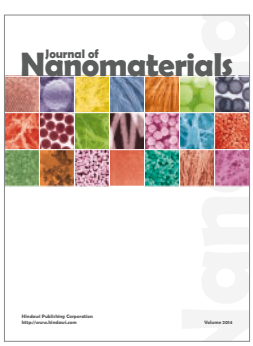


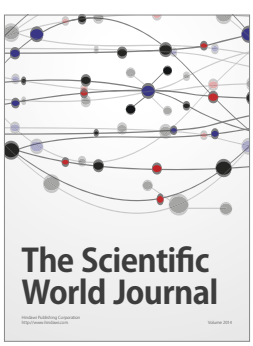




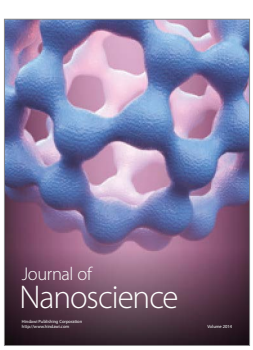




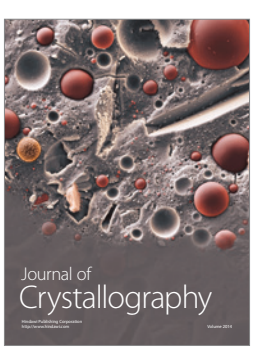




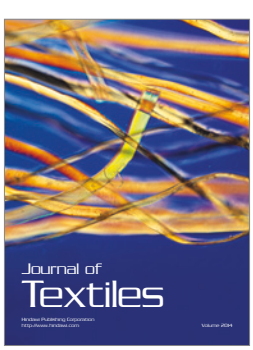












Hindawi

Submit your manuscripts at
https://www.hindawi.com

Copyright of Advances in Materials Science & Engineering is the property of Hindawi Limited and its content may not be copied or emailed to multiple sites or posted to a listserv without the copyright holder's express written permission. However, users may print, download, or email articles for individual use.